

# LONGITUDINAL BUNCH SHAPING WITH DOUBLE DOGLEG BASED EMITTANCE EXCHANGE BEAM LINE\*

John G. Power<sup>1#</sup>, Alexander Zholents<sup>1</sup>, Kwang-Je Kim<sup>1</sup>, Manoel Conde<sup>1</sup>, Wei Gai<sup>1</sup>, Chunguang Jing<sup>1,2</sup>, Moohuun Cho<sup>3</sup>, Won Namkung<sup>3</sup>, Gwanghui Ha<sup>1,3</sup>

<sup>1</sup> Argonne National Laboratory, Argonne, IL 60439, USA

<sup>2</sup> Euclid Techlabs, LLC, Solon, OH, USA

<sup>3</sup> POSTECH, Pohang 790-784, KOREA

## Abstract

A new program is under development at Argonne National Laboratory (ANL) to use an emittance exchange (EEX) beamline to produce longitudinally shaped electron bunches. While the ultimate goal is to generate triangular shapes optimized for high transformer ratio wakefield acceleration, we will begin by studying the basic capability of the double dogleg EEX beamline to control the bunch shape. We are studying effects that degrade the quality of the longitudinal current profile including: non-uniform particle distribution, emittance, the deflecting cavity thick-lens effect, 2<sup>nd</sup> order effects, space charge effects and coherent synchrotron radiation effects. We present the double dogleg EEX beamline layout and the diagnostic design as well as give a progress report on the experimental status of the program.

## EMITTANCE EXCHANGE BASED BUNCH SHAPING

Emittance exchange (EEX) based bunch shaping is one of leading approaches for controlling current profiles. A fundamental property of the EEX is that longitudinal properties at the exit are governed by horizontal properties at the entrance [1]. In the linear regime, this property gives a linear relationship between the longitudinal position at the exit and the horizontal position at the entrance.

$$z_f = [k\xi - s\{\eta + k\xi(L + D)\}]x_i, \quad (1)$$

where  $k$  is the transverse deflecting cavity (TDC) kick strength,  $\xi$  is the  $R_{56}$  term of dogleg,  $\eta$  is the  $R_{16}$  term of dogleg,  $L$  is the  $R_{12}$  term of dogleg,  $D$  is the drift length between the dipole magnet and TDC, and  $s$  is the  $x$ - $x'$  slope at the entrance. This equation means that final current profile can be controlled by manipulating initial horizontal profile. Due of the relationship given in Eq. (1), EEX based bunch shaping can generate arbitrary current profiles including: microbunch train, trapezoid profile, triangle profile, double triangle profile etc. Although many different approaches for shaping have been suggested and successfully demonstrated [2-5], EEX based bunch shaping has not been demonstrated yet.

To achieve high-resolution, arbitrary-current profiles

using EEX, we must first understand the factors that limit the shaping capability and then identify ways to mitigate the distortions. Our studies revealed several effects which degrade the shaping including: non-zero emittance, thick-lens effect from TDC, higher order effects from non-linear fields, space charge effect, and coherent synchrotron radiation (CSR). We found that these degradation effects could be reduced by manipulating the initial transverse and longitudinal phase spaces. Since the final current profile is determined by initial transverse properties in EEX beamline, most of non-linear field effects in the current profiles are closely related to the initial transverse properties. Initial longitudinal properties are also important factors because they determine the bunch length before the second dogleg which determines the strength of space charge effect and CSR.

Argonne National Laboratory (ANL) has a new program to generate high-resolution arbitrary current profiles using EEX. This experiment has three objectives. First, several current profiles will be generated to study the shaping capability of the EEX method. Second, final current profiles will be measured while the initial conditions are varied to clarify the source of distortion and to study the mitigation method. Third, the transport matrix of the EEX beamline will be measured and compared with the transport matrices calculated from theory. Since the measured transport matrix includes the space-charge effect and CSR, comparisons with well-known linear and second order matrices will reveal those effects thoroughly.

For the experiment, the 15-MeV rf photoinjector at the Argonne Wakefield Accelerator (AWA) facility is used to generate a high charge beam and control the longitudinal chirp. At the end of the photoinjector, an EEX and diagnostic beamline are installed (Fig. 1). Here we present the overall beamline layout and the design consideration for each specific section.

## INJECTOR SECTION

The drive beam determines two figures of merit in a dielectric wakefield accelerator (DWA). One is the transformer ratio which determines the energy transfer efficiency from the drive beam to the witness beam and the other is the accelerating gradient which determines the total length of the linac. These two parameters are closely related to the current profile and the charge of the drive beam. We choose the drive beam charge as 1-2 nC which

\*Work supported by High Energy Physics, Office of Science, USDOE

#jp@anl.gov

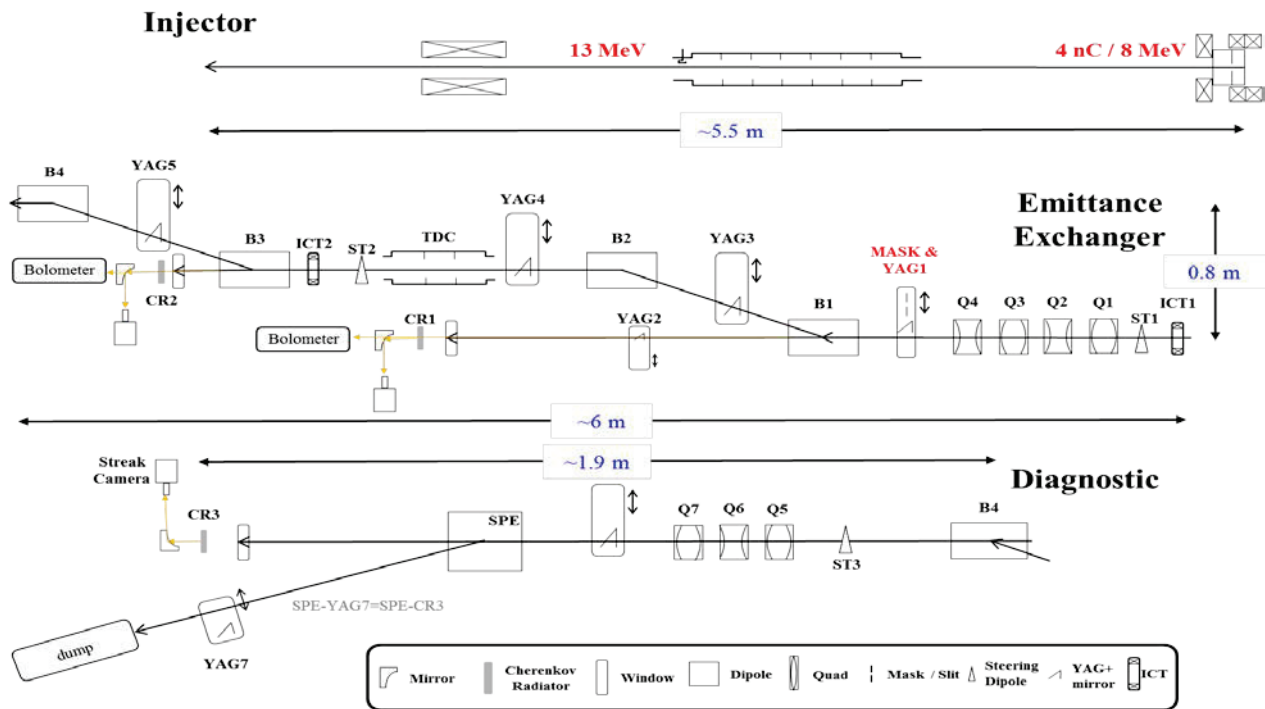


Figure 1: Schematics of AWA beamline for proof-of-principle experiment of EEX based bunch shaping.

can generate around 100 MV/m, a result that can be used in practical applications. Since EEX based bunch shaping loses almost half of the initial charge at the transverse mask, the electron gun should generate the charge of 4 nC. A 1.3 GHz RF photocathode gun is used to generate 4 nC and accelerate it to 8 MeV. A subsequent accelerating cavity further accelerates it to ~13 MeV.

One of the important functions of the injector section is to impart a longitudinal chirp. The area between B2 and B3 is critical if we consider the space charge effect and CSR. Since these collective effects mostly affect the current profile in this region, one should keep the bunch length of the beam large in order to reduce these effects. The bunch length in this region fully depends on the longitudinal chirp at the entrance of EEX beam line. In the experiment, the longitudinal chirp will be controlled by adjusting accelerating cavity phase which allows us to identify the relationship between the longitudinal chirp and the collective effects.

### EEX SECTION

Simulations reveal that second order terms in the transport matrix significantly distort the final current profile. However, since the final current profiles depend on the initial horizontal properties, then the horizontal properties are can be used to mitigate the distortion induced by the non-linear fields. We found that the second order effect can be mitigated by applying an appropriate  $x-x'$  and  $y-y'$  slopes at the entrance. To achieve this mitigation, four quadrupoles were placed in front of the transverse mask to control all transverse parameters simultaneously.

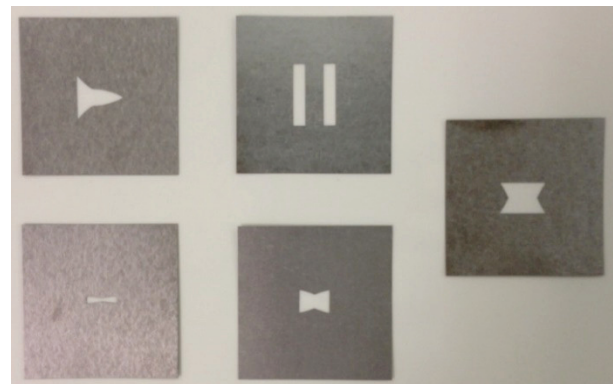


Figure 2: Tungsten mask to chop the beam transversely.

To confirm the shaping capability of EEX based method, a few different profiles have to be generated. The shape of the final current profile depends on the shape of the transverse mask. We prepared three different masks which generate the same horizontal profile with different charges, one mask for matrix measurement and another mask to generate three different profiles as shown in Fig. 2. 250  $\mu\text{m}$  thick tungsten plates are used as masks and they are cut by laser. The shape of the mask is determined by Eq. 2 with the particle distribution from the simulation.

$$g(x) = 2 \int_0^{f(x)} N(x, y) dy, \quad (2)$$

where  $g(x)$  is the desired profile,  $f(x)$  is the mask shape and  $N(x, y)$  is the particle distribution.

Shaped bunches enter the double dogleg EEX structure which is the fundamental EEX structure suggested in [1].

Content from this work may be used under the terms of the CC BY 3.0 licence (© 2014). Any distribution of this work must maintain attribution to the author(s), title of the work, publisher, and DOI.

This structure includes four rectangular bending magnets which provide 20 degree bending and TDC. Main parameters for EEX beam line are given in Table 1.

Table 1: Beamline Parameters for EEX Beamline

| Beamline parameters                 | Value | Unit            |
|-------------------------------------|-------|-----------------|
| Bending angle                       | 20    | degree          |
| Length of dipole magnet             | 30    | cm              |
| Drift between dipole magnet         | 86    | cm              |
| Drift between dipole magnet and TDC | 50    | cm              |
| TDC kick strength                   | 2.24  | m <sup>-1</sup> |
| Length of TDC                       | 48    | cm              |

### DIAGNOSTIC SECTION

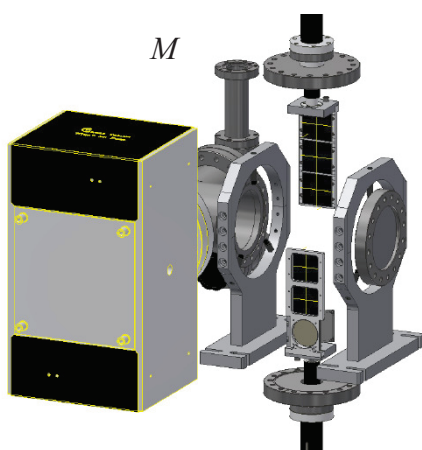


Figure 3: YAG and mask mounting system design.

### Control Variable Measurement

The beam size at the mask position will be measured using a YAG screen mounted on the 8" actuator with the masks. We use two 8" actuators in the single cross to hold a YAG screen and five masks simultaneously as shown in Fig. 3. To measure both x-x' and y-y' slopes, another two screens, YAG2 and CR1, are located in the straight section behind B1 to apply a three screen measurement. Bunch length is measured to clarify the relationship between the bunch length in B2-B3 and collective effects. To measure the bunch length, Cherenkov radiators are placed out of the vacuum chamber but close to the window. Cherenkov radiation from this radiator will be guided to the streak camera using plane or parabolic mirrors. Also, relative CSR strength behind B1 and B3 will be estimated using a bolometer.

### Current Profile Measurement

Cherenkov radiators and the streak camera are also used to measure the current profile. Since the streak camera has the resolution of ~2 ps, final bunch length is designed to ~10 ps. Due to this tight resolution limit, both

geometric and chromatic aberrations on the optical system are critical. Since the Cherenkov radiator generates severe geometric aberration, aerogel is chosen instead of quartz because of its low refractive index. Most test procedures follows the contents in [6]. Also, we considered a few different optical guide lines to minimize temporal lengthening as shown in Fig. 4. They will be experimentally tested and the one showing the best performance will be used.

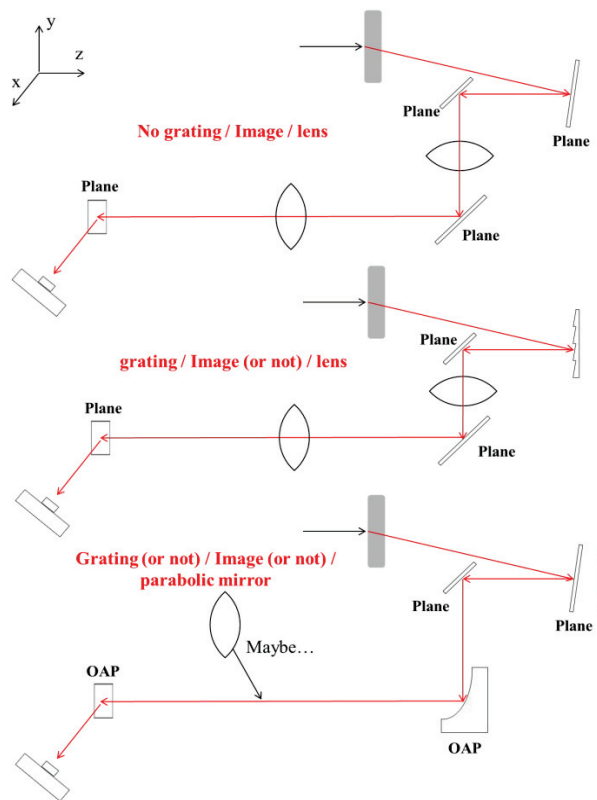


Figure 4: Configurations of optical guide line.

### Transport Matrix Measurement

To measure the transport matrix, the beam should be separated into four small segments. For the transverse phase space, the top-middle mask in the Fig. 2 will be used to make two beams. For the longitudinal phase space,  $\alpha$ -BBO crystal will be used to generate two bunches which are close to each other. Each transport matrix elements can be estimated by manipulating x-x' slope and longitudinal chirp with these four segments.

### REFERENCES

- [1] P. Emma, Phys. Rev. ST Accel. Beams 9, 100702 (2006).
- [2] M. Cornacchia, Phys. Rev. ST Accel. Beams 9, 120701 (2006).
- [3] C. Jing et al., Phys. Rev. Lett 98, 144801 (2007).
- [4] R. England, Phys. Rev. Lett. 100, 214802 (2008).
- [5] P. Piot, Phys. Rev. Lett. 108, 034801 (2012).
- [6] J. Bahr, Nucl. Instr. and Meth. A 538, 597-607 (2005).